Supplementary Information

First Principles Study of Two-dimensional Li_3CX (X=S, Se) Monolayers for Hydrogen Storage

Sangeeta Meena, Ramandeep Singh, Nidhi Verma and Ashok Kumar*

Department of Physics, Central University of Punjab, Bathinda, 151401, India

(November 26, 2025)

*Corresponding Author: ashokphy@cup.edu.in

Relaxed position coordinates the studied structures

POSCAR
Li3CS
1.00000000000000
3.7743710626556193 0.0000000000032687 0.0000000000000000
-1.8871855312718635 3.2687012235396891 -0.0000000000000000
0.0000000000000002 0.0000000000000000 39.9455876635080855
Li C S
3 1 1
Direct
0.0000000000000000 0.0000000000000000 0.4601253642670785
-0.0000000000000000 -0.0000000000000000 0.5434696754224304
0.6666666670000012 0.3333333300000021 0.4926677709818933
0.3333333329999988 0.6666666670000012 0.4788981585958270
0.3333333329999988 0.6666666670000012 0.5248390307327637

POSCAR
Li3CSe
1.00000000000000
3.8844058756971465 0.0000000000045271 -0.0000000000000001
-1.9422029377899888 3.3639941669319602 0.0000000000000003
-0.0000000000000015 0.0000000000000016 32.7864124228550651
Li C Se
3 1 1
Direct
-0.0000000000000000 0.0000000000000000 0.4506058043674540
0.0000000000000000 -0.0000000000000000 0.5583565674494446
0.6666666670000012 0.3333333300000021 0.4877869184892805
0.3333333329999988 0.6666666670000012 0.4709849987189612
0.3333333329999988 0.6666666670000012 0.5322657109748528

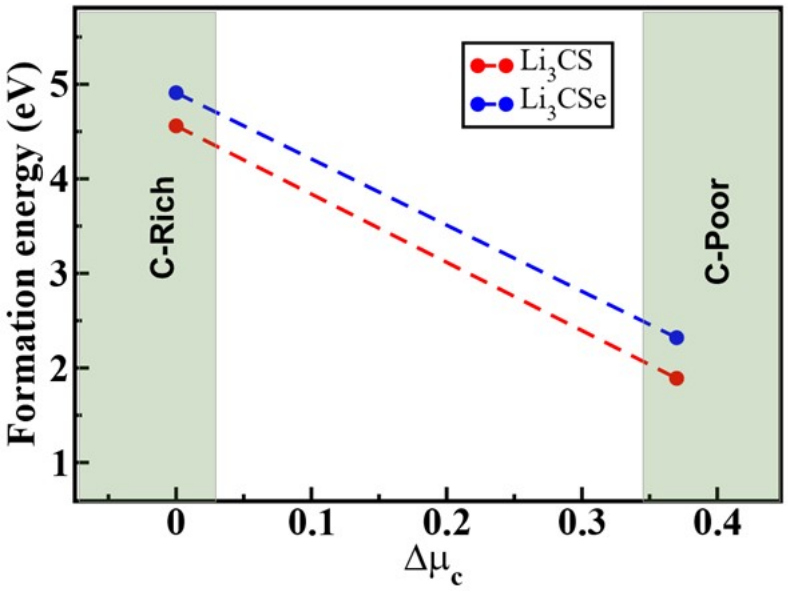

Figure S1. Phase diagram illustrating the attempted derivation of Li_3CX from Li_3X_2. The formation energies remain positive across the chemical potential range, indicating that this route is energetically unfavourable compared to the Li_3C_2 pathway.

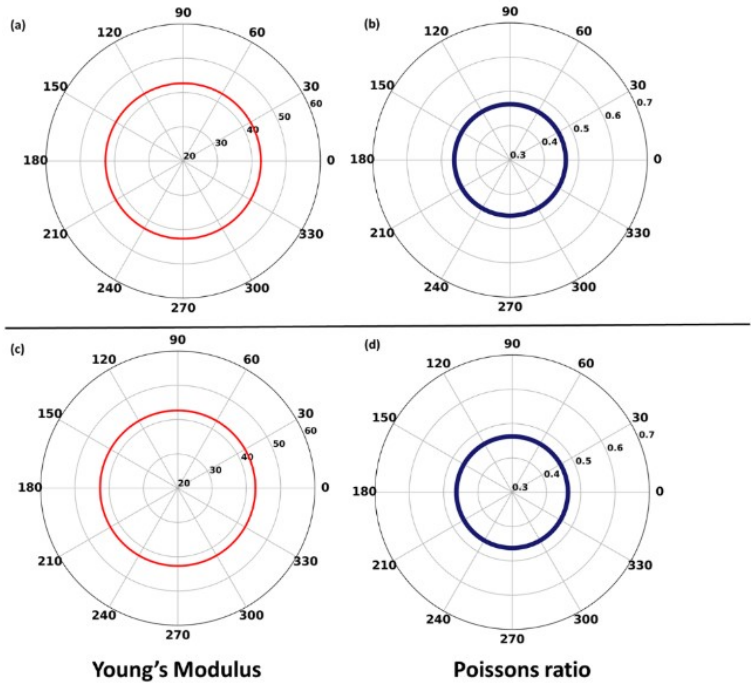

Figure S2. Polar plots comparing the mechanical anisotropy of Li_3CS and Li_3CSe structures. Panels (a) and (b) depict the directional dependence of Young's modulus and Poisson's ratio for Li_3CS, respectively, while panels (c) and (d) show the corresponding properties for Li_3CSe.

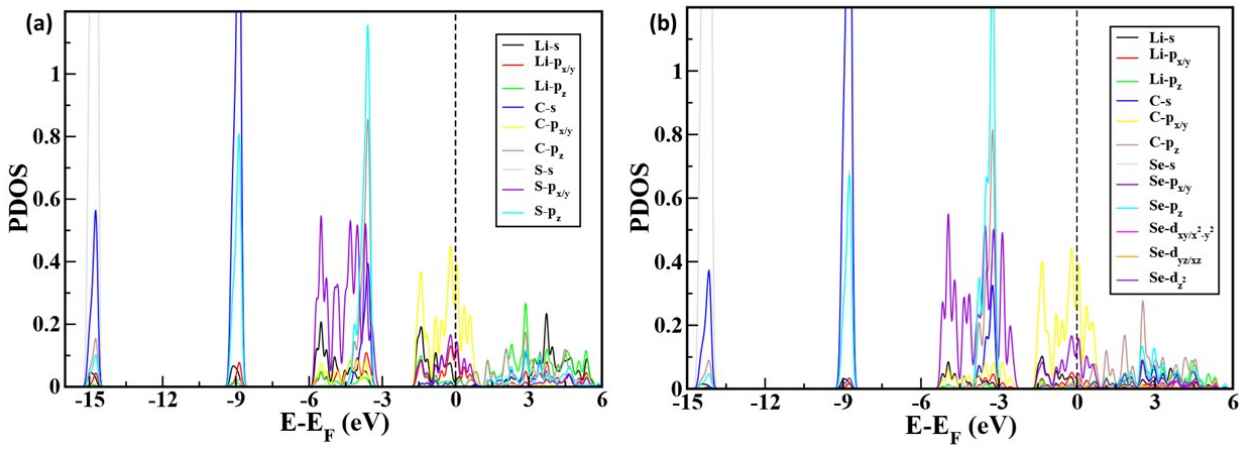

Figure S3. Orbital-resolved partial density of states (PDOS) for Li, C, S, and Se atoms in the Li_3CX monolayers (X = S in panel (a), Se in panel (b)).

Table S1. Possible sites of the lower and upper sides of the Li_3CX monolayers

Up-side		**Down-side**	
Adsorption Site	**Adsorption Energy (eV)**	**Adsorption Site**	**Adsorption Energy (eV)**
Li_3CS			
U_1	−1.08	**D_1**	−1.1
U_2	−1.04	**D_2**	−1.04
U_3	−1.09	**D_3**	−1.09
U_4	−1.08	**D_4**	−1.08
U_5	−1.09	**D_5**	−1.19
Li_3CSe			
U_1	-1.13	**D_1**	-1.18
U_2	-1.27	**D_2**	-1.12
U_3	-1.18	**D_3**	-1.20
U_4	-1.26	**D_4**	-1.25
U_5	1.27	**D_5**	-1.27

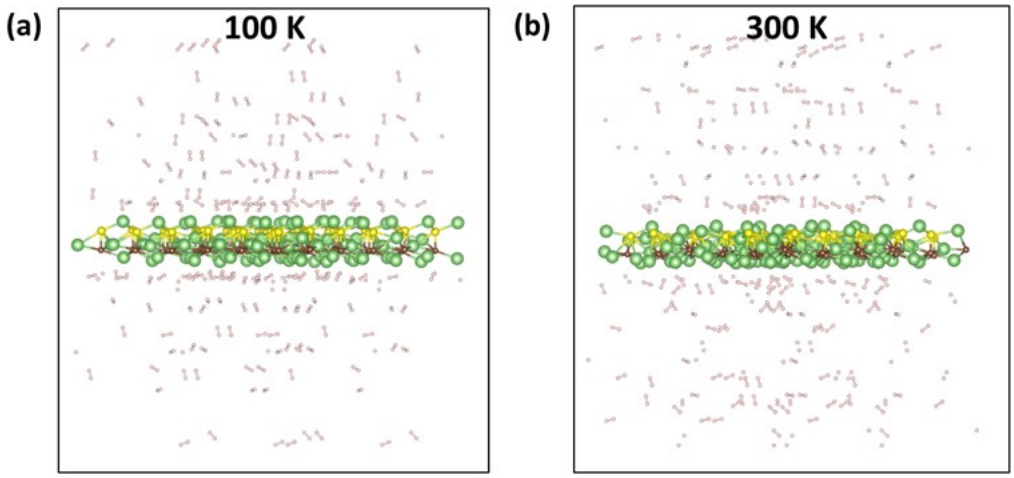

Figure S4. Snapshots of ab initio molecular dynamics simulations for the H_2 absorbed Li_3CS monolayer at (a) 100 K and (b) 300 K.

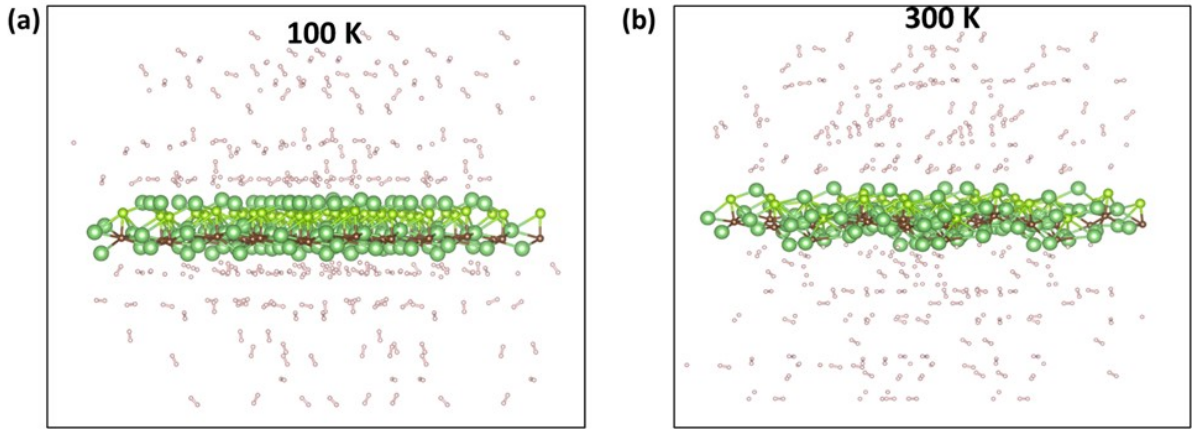

Figure S5. Snapshots of ab initio molecular dynamics simulations for the H_2 absorbed Li_3CSe monolayer at (a) 100 K and (b) 300 K.

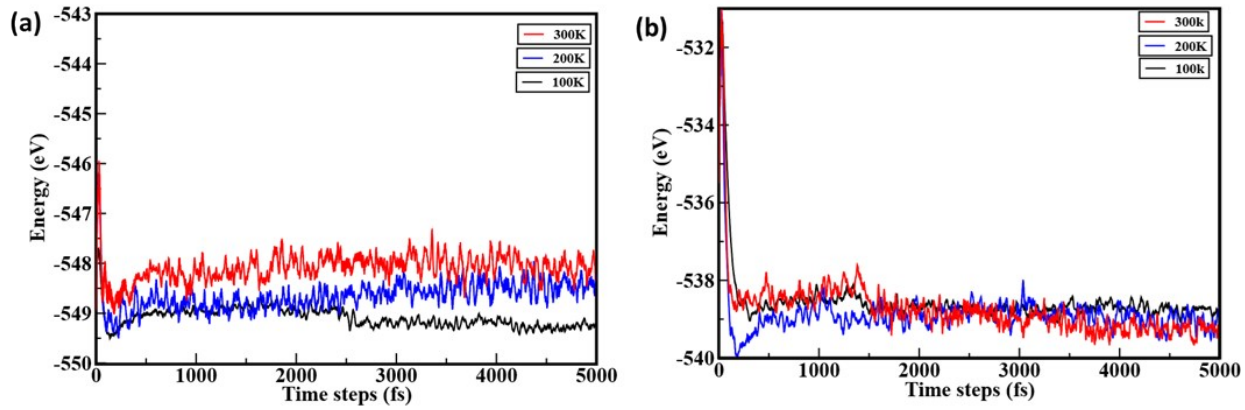

Figure 6: AIMD simulations depicting hydrogen release behavior of **(a)** $6H_2@Li_3CS$ and **(b)** $6H_2@Li_3CSe$ monolayer at 100 K, 200K and 300 K.

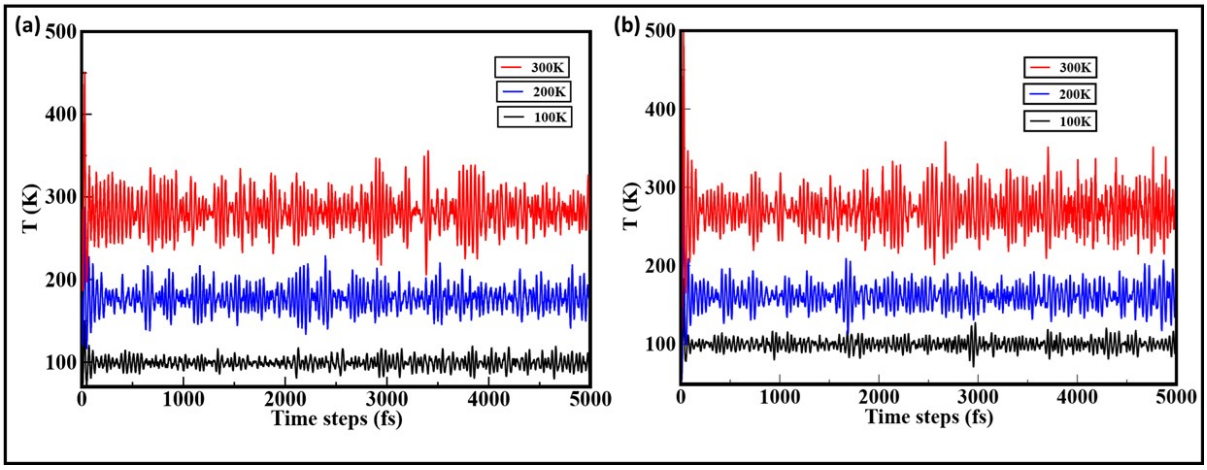

Figure S7. Temperature fluctuations of the $6H_2@Li_3CS$ and $6H_2@Li_3CSe$ monolayer at 100 K, 200K and 300 K.

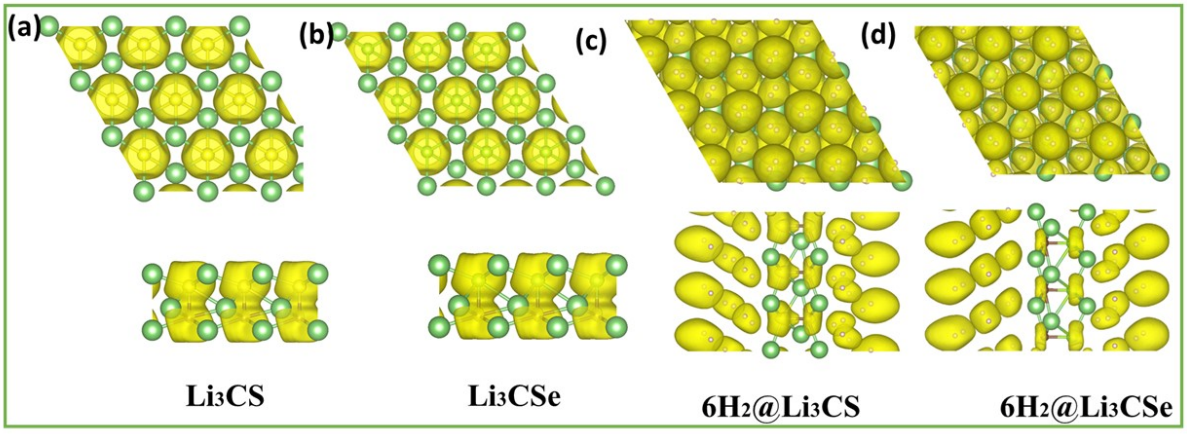

Figure S8. (a, b) ELF plots for pristine Li_3CX monolayers. **(c, d)** ELF plots for six H_2 molecules adsorbed Li_3CX monolayers.

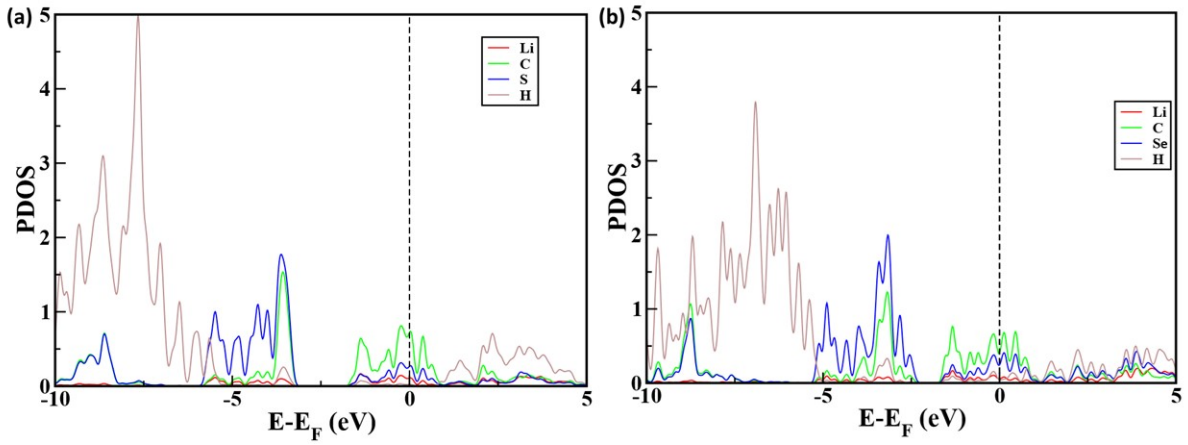

Figure S9. Partial density of states (PDOS) for the Li_3CX monolayers with six adsorbed H_2 molecules.

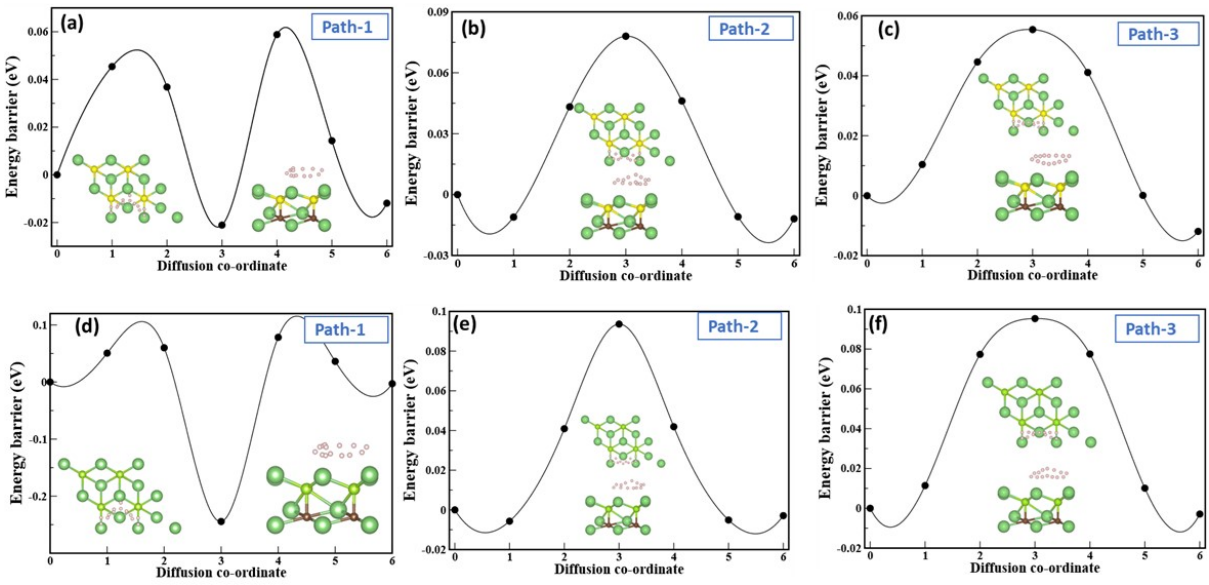

Figure S10. Climbing-image nudged elastic band (CI-NEB) energy profiles for hydrogen diffusion on the S- or Se-side of the Li_3CX monolayer.

Table S2: CI-NEB-calculated hydrogen diffusion barriers (in eV) along three representative paths below and above the Li_3CS and Li_3CSe monolayer surfaces.

Diffusion paths	**Bleow Li_3CS surface (C-side) (eV)**	**Above Li_3CS surface (S-side) (eV)**	**Bleow Li_3CSe surface (C-side) (eV)**	**Above Li_3CSe surface (Se-side) (eV)**
Path-1	0.0674	0.0588	0.0781	0.0783
Path-2	0.0604	0.0780	0.080	0.093
Path-3	0.0790	0.0554	0.095	0.0953